antioxidants

MDPI

Article

The Protective Effects of α-Mangostin Attenuate Sodium Iodate-Induced Cytotoxicity and Oxidative Injury via Mediating SIRT-3 Inactivation via the PI3K/AKT/PGC-1α Pathway

Chen-Ju Chuang [1,†], Meilin Wang [2,†], Jui-Hsuan Yeh [3], Tzu-Chun Chen [3], Shang-Chun Tsou [4], Yi-Ju Lee [5], Yuan-Yen Chang [2,*] and Hui-Wen Lin [6,7,*]

1 Emergency Department, Kaohsiung Municipal United Hospital, Kaohsiung 80457, Taiwan; ilovespurs168@gmail.com
2 Department of Microbiology and Immunology, School of Medicine, Chung Shan Medical University and Clinical Laboratory, Chung Shan Medical University Hospital, Taichung 40201, Taiwan; wml@csmu.edu.tw
3 Institute of Medicine, Chung Shan Medical University, Taichung 40201, Taiwan; simon855264@gmail.com (J.-H.Y.); cherish4488@gmail.com (T.-C.C.)
4 Department of Nutrition, Chung Shan Medical University, Taichung 40201, Taiwan; eq7bie5d@gmail.com
5 Department of Pathology, Chung-Shan Medical University, Chung-Shan Medical University Hospital, Taichung 40201, Taiwan; jasmine.lyl@gmail.com
6 Department of Optometry, Asia University, Taichung 41354, Taiwan
7 Department of Medical Research, China Medical University Hospital, China Medical University, Taichung 40402, Taiwan
* Correspondence: cyy0709@csmu.edu.tw (Y.-Y.C.); d9138001@asia.edu.tw (H.-W.L.); Tel.: +886-4-24730022 (ext. 12028)
† These authors have contributed equally to this work and share the first authorship.

Citation: Chuang, C.-J.; Wang, M.; Yeh, J.-H.; Chen, T.-C.; Tsou, S.-C.; Lee, Y.-J.; Chang, Y.-Y.; Lin, H.-W. The Protective Effects of α-Mangostin Attenuate Sodium Iodate-Induced Cytotoxicity and Oxidative Injury via Mediating SIRT-3 Inactivation via the PI3K/AKT/PGC-1α Pathway. *Antioxidants* **2021**, *10*, 1870. https://doi.org/10.3390/antiox10121870

Academic Editors: Raul Rodrigues-Diez, Beatriz Suárez-Álvarez and Lucas Matias Opazo-Ríos

Received: 24 September 2021
Accepted: 19 November 2021
Published: 24 November 2021

Abstract: It is well known that age-related macular degeneration (AMD) is an irreversible neurodegenerative disease that can cause blindness in the elderly. Oxidative stress-induced retinal pigment epithelial (RPE) cell damage is a part of the pathogenesis of AMD. In this study, we evaluated the protective effect and mechanisms of alpha-mangostin (α-mangostin, α-MG) against $NaIO_3$-induced reactive oxygen species (ROS)-dependent toxicity, which activates apoptosis in vivo and in vitro. MTT assay and flow cytometry demonstrated that the pretreatment of ARPE-19 cells with α-MG (0, 3.75, 7.5, and 15 μM) significantly increased cell viability and reduced apoptosis from $NaIO_3$-induced oxidative stress in a concentration-dependent manner, which was achieved by the inhibition of Bax, cleaved PARP-1, cleaved caspase-3 protein expression, and enhancement of Bcl-2 protein. Furthermore, pre-incubation of ARPE-19 cells with α-MG markedly inhibited the intracellular ROS and extracellular H_2O_2 generation via blocking of the abnormal enzyme activities of superoxide dismutase (SOD), the downregulated levels of catalase (CAT), and the endogenous antioxidant, glutathione (GSH), which were regulated by decreasing PI3K-AKT-PGC-1α-STRT-3 signaling in ARPE-19 cells. In addition, our in vivo results indicated that α-MG improved retinal deformation and increased the thickness of both the outer nuclear layer and inner nuclear layer by inhibiting the expression of cleaved caspase-3 protein. Taken together, our results suggest that α-MG effectively protects human ARPE-19 cells from $NaIO_3$-induced oxidative damage via antiapoptotic and antioxidant effects.

Keywords: age-related macular degeneration (AMD); oxidative stress; retinal pigment epithelial (RPE); alpha-mangostin (α-MG); antiapoptotic; antioxidant

1. Introduction

Retinal pigmented epithelial cells (RPEs) are located between photoreceptor cells (cone and rod cells) and Bruch's membrane [1]. RPEs are highly metabolically active and sensitive to oxidative stress when the retina is exposed to many reactive oxygen species

(ROS) [2]. However, abnormal RPEs are regarded as playing an important role in age-related macular degeneration (AMD), a disease that results in irreversible center vision loss in the elderly population. This disease can generally be divided into two categories: dry AMD and wet AMD. The former is characterized by accumulation of drusen in the retina, thickening of Bruch's membrane, RPE cell and photoreceptor dysfunction, and severe abnormal neovascularization (angiogenesis), which grows into the central region of the retina, leading to retinal exudation, hemorrhage, and, eventually, serious impairment of vision [3,4]. At present, due to the clinical application of anti-vascular endothelial growth factor (VEGF) agents, wet AMD can be effectively controlled. However, the underlying mechanism of the pathology of dry AMD is still largely unknown. Therefore, there are currently no effective treatment options for dry AMD.

In cellular systems, the generation of reactive oxygen species (ROS) can cause cell damage and affect the structure and function of membrane lipids, proteins, and nucleic acids [5]. ROS is considered to be an important mechanism that leads to a variety of neurodegenerative diseases, such as AMD. Previous studies have demonstrated that inhibiting ROS-induced RPE cell damage may inhibit AMD progression [6–8]. Catalase, superoxide dismutase (SOD), and glutathione (GSH) are major enzymes that protect RPE cells through increased expression by effectively scavenging ROS and attenuating oxidative damage [9].

PGC-1α, PGC-1β, and PRC (PGC-1-related coactivator) belong to the peroxisome proliferator-activated receptor gamma coactivator-1 (PGC-1) family. They can regulate the biogenesis and respiratory function of mitochondria as well as targeting the mitochondrial antioxidant defense system [10]. The role of PGC-1α is to serve as a switch between mitochondrial biogenesis and oxidative damage by controlling the mitochondrial levels of ROS. Loss-of-function studies of PGC-1α have shown bursts of ROS and an increase in mitochondrial damage and degradation, whereas gain-of-function enhanced mitochondrial biogenesis and the expression of mitochondrial antioxidant defense system-related genes, such as SOD2 (superoxide dismutase 2) and TRX1 (thioredoxin) [10]. However, both pathways, mitochondrial biogenesis and ROS control, strive for the preservation of mitochondrial homeostasis. Post-translational modification of the energy sensors, AMPK (AMP-activated protein kinase), and SIRT-1/3 (sirtuin-1/3), which induce autophagy, are known to regulate PGC-1α activities [11]. In RPE cells, PGC-1α has been shown to drive mitochondrial biogenesis and to activate the antioxidant defense system [8,12]. Recent studies have reported that SOD2 is a major downstream signal of SIRT-3-mediated mitochondrial $O2^{\bullet -}$ reduction, and deacetylation of SOD2 by the SIRT-3 pathway regulates SOD2 enzymatic activity [13]. We therefore hypothesized that $NaIO_3$ might induce mitochondrial ROS in RPE cells and that scavenging mitochondrial ROS could be an effective strategy for preventing $NaIO_3$-induced retinal toxicity.

Mangosteen (known as the "Queen of Fruit"), which is edible and also known to have medicinal properties, is generally cultivated in Southeast Asia [14]. The major bioactive secondary metabolites of mangosteen have been found to be xanthone derivatives, including α, β, and γ mangostin. Alpha-mangostin (α-MG) has antiinflammatory [15,16], antibacterial [17,18], antioxidant [19], anticancer [20,21], and cardioprotective [22] activities both in vitro and in vivo. α-MG possesses strong antioxidant activity that has gradually been confirmed in recent years. The researchers found that α-MG displayed the ability to scavenge ROS in each dose [23]. Márquez-Valadez and coworkers (2009) found that α-MG could be considered an accurate antioxidant/neuroprotective tool to be employed in further paradigms of neuronal cell damage [24]. Although α-MG has shown a variety of antioxidant and protective properties, its effects on retina health have not yet been clarified. In this study, we will evaluate whether α-MG may reduce or prevent $NaIO_3$-induced retinal damage both in vitro and in vivo.

2. Materials and Methods

2.1. Cell Culture

The ARPE-19 cell line was purchased from the American Type Culture Collection (Manassas, VA, USA). The cells were cultured in Dulbecco's modified Eagle medium (DMEM) supplemented with 10% heat inactivated fetal bovine serum (FBS) (Gibco; Thermo Fisher Scientific, Inc., Waltham, MA, USA), 100 µg/mL streptomycin and 100 U/mL penicillin (CSPC Pharmaceutical Group Ltd., Shijiazhuang, China) at 37 °C in an atmosphere containing 5% CO_2. The cells were passaged every three days once grown to ~90% confluence.

2.2. Cell Viability Assay

ARPE-19 cells (1.5×10^5 cells/well) were seeded into 24-well plates at 1 mL volume and incubated at 37 °C for 24 h. The culture medium was subsequently replaced by a medium containing various doses of α-MG (0, 3.75, 7.5, and 15 µM) alone or with a co-treatment of $NaIO_3$ for 24 h. For the cell viability assay condition and procedure, refer to [25].

2.3. Measurement of Intracellular ROS Production

The effect of different concentrations of α-MG (0, 3.75, 7.5, and 15 µM) on $NaIO_3$-induced intracellular ROS generation in ARPE-19 cells was further confirmed by flow cytometry (BD Biosciences, San Jose, CA, USA), using DCFH-DA fluorogenic dye as a probe. Data analysis was performed using CellQuest.

2.4. Measurement of Mitochondrial Damage

For the analysis of mitochondrial status, the cells were incubated with JC-1 dye (2 µg/mL; Cayman Chemical, Ann Arbor, MN, USA) for 50 min. Two µL of Hoechst33342, a DNA-specific fluorescent dye, was added, and the cells were incubated in darkness at 37 °C for 10 min. For the conditions and procedure, refer to [25].

2.5. Measurements of Antioxidative Capacities and Extracellular H_2O_2 Production

The effects of different concentrations of α-MG (pretreatment 0, 3.75, 7.5, 15 µM) on the $NaIO_3$-induced antioxidative capacities and H_2O_2 generation in ARPE-19 cells were further confirmed by ELISA kits. The activities of superoxide dismutase (SOD), catalase (CAT), and reduced glutathione (GSH) were analyzed using ELISA kits from Cayman according to the manufacturer's instructions (Cat. 706002, 707002, and 703002, Cayman, Ann Arbor, MI, USA). The extracellular H_2O_2 production was determined using a Biovision assay kit (Biovision Research Products, Milpitas, CA, USA) following the manufacturer's instructions.

2.6. Western Blotting

The ARPE-19 cells were pretreated under different conditions for 24 h and, after the incubation of cell lysates with different primary antibodies including Bcl2 (ab182858) purchased from abcam (Cambridge, UK), Bax (2D2), cleaved caspase-3 (31A1067), cleaved PARP-1 (194C1439), PI3K-p110 (H-239), p-AKT (B-5), PGC-1α (D-5), SIRT-3, and GAPDH (6C5) purchased from Santa Cruz (Santa Cruz, CA, USA), and SIRT-3 (D22A3) purchased from Cell Signaling (Beverly, MA, USA) primary antibodies, immunoblotting was performed, as described previously in [16].

2.7. Animal Model

Eight-week-old BABL/c mice were purchased from the Asia University Animal Care and Use Committee (IACVC No. 107-a51a-20, 01 August 2019) and housed in standard cages with a 12-h light–dark cycle. The mice were randomly divided into three groups with each group containing six mice:

1. Mock group: Animals pretreated with an intraperitoneal (IP) injection of PBS and then a single intravenous (IV) injection of PBS.
2. Vehicle-treated group: Animals pretreated with an IP injection of PBS and then a single IV injection of 40 mg/kg $NaIO_3$ [26].
3. Experimental group: Animals pretreated with an IP injection of 20 mg/kg α-MG and then a single IV injection of 40 mg/kg $NaIO_3$ [27].

2.8. Histology and Immunohistochemistry

The mice were sacrificed, and both eyes were surgically collected and applied to the Davidson's solution (containing 10% formalin, 10% glacial acetic acid, and 4% formaldehyde) to fix the specimen for three days [28]. Eyeball tissues were embedded in paraffin before sectioned at 5 μm-thick and stained with hematoxylin and eosin (H&E) to capture the tissue section image via optical microscope (Olympus Optical, Tokyo, Japan). Different retinal thickness, i.e., whole retina, inner nuclear layer (INL), and outer nuclear layer (ONL) were randomly measured 6 times from the inferior and superior hemiretina in the range of 600–900 μm on nasal and temporal side of the optic nerve.

Besides the expression of caspase-3 in mice retina evaluated by Image J Immunohistochemistry Toolbox (National Institute of Health, Starkville, MD, USA), the tissue sections were incubated with cleaved caspase-3 (1:100, Cell Signaling Technology, Danvers, MA, USA) antibody in BondMax automated slide staining system (Vision BioSystems Ltd., Newcastle Upon Tyne, UK) and the tissue section image screenshotted.

2.9. Retinal Imaging

Optical coherence tomography (OCT) was performed using RTVue XR Avanti with AngioVue (Optovue Inc, Fremont, CA, USA). Briefly, OCT of a certain region of the retina was performed repeatedly, and the resultant scans were examined for changes [27].

2.10. Statistical Analysis

All grouping and subject selection in this study were decided completely at random. All data were analyzed in SPSS software. Multiple group comparisons were performed using one-way ANOVA followed by least significant difference (LSD) post hoc test. $p < 0.05$ indicated statistical significance for all tests. The values of the results were representative in terms of the mean ± standard deviation (SD).

3. Results

3.1. α-Mangostin (α-MG) Protects ARPE-19 from $NaIO_3$-Induced Damage

To confirm the cytotoxicity of α-MG on ARPE-19, the cells were pretreated with α-MG (0, 3.75, 7.5, and 15 μM) alone or with a co-treatment of $NaIO_3$. After 24 h, the cell viability of ARPE-19 was assessed using an MTT assay. The cell survival rate was unaffected following the treatment of cells with < 15 μM α-MG (Figure 1A). However, treatment with 20 μM α-MG significantly reduced the cell viability, with the effects being significantly different from the untreated controls (0 μM). For this reason, <15 μM α-MG was used for all subsequent experiments.

We also evaluated whether α-MG treatment could reduce ARPE-19 cell damage induced by $NaIO_3$. Before being treated with $NaIO_3$ (6 mM), the ARPE-19 cells were pretreated with α-MG (3.75, 7.5, and 15 μM) for 1.5 h. Based on the results, significantly increased protective effects were found on cell death, compared with the group treated with $NaIO_3$ only (Figure 1B).

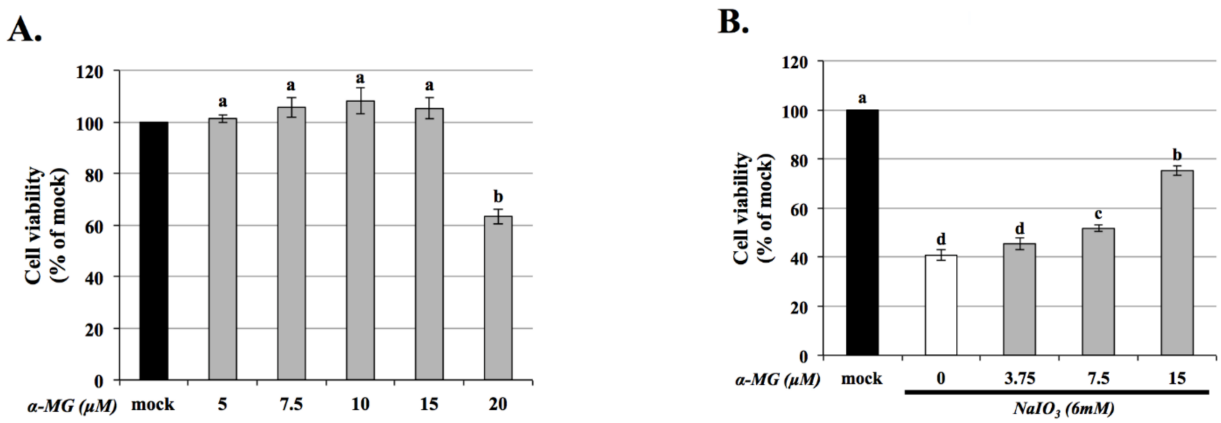

Figure 1. α-MG attenuates $NaIO_3$-induced cytotoxicity in ARPE-19 cells. (**A**) ARPE-19 cells were treated with different concentrations of α-MG (5, 7.5, 10, 15, and 20 μM) for 24 h. (**B**) Effect of α-MG against $NaIO_3$-induced cytotoxicity in ARPE-19 cells. Before being $NaIO_3$ (6 mM) treated, three different concentrations of α-MG (3.75, 7.5, and 15 μM) were pretreated with ARPE-19 cells for 1.5 h, and, after 24 h, the cell viability was measured using a CCK-8 assay. Data were expressed by mean ± SD (n = 3). Values without a common superscript letter are significantly different ($p < 0.05$).

3.2. Treatment with α-MG Suppressed $NaIO_3$-Induced Mitochondrial Dysfunction

The JC-1 staining assay is used to evaluate the function of mitochondria [29]. JC-1 monomers emit green fluorescence and indicate damaged mitochondria, while JC-1 polymers emit red fluorescence and indicate healthy mitochondria. The treatment of ARPE-19 cells with $NaIO_3$ for 24 h caused the accumulation of JC-1 monomers in the mitochondria, which was reduced in a dose-dependent manner following treatment with various concentrations of α-MG (0, 3.75, 7.5, and 15 μM). (Figure 2A). Quantitative data revealed that the green/red fluorescence ratio and $NaIO_3$-induced mitochondrial damage increased following treatment with $NaIO_3$ and improved following treatments with α-MG (Figure 2B). The results indicated that $NaIO_3$-induced mitochondrial dysfunction was improved via the inhibition of mitochondrial fission, but α-MG can alleviate this appearance.

3.3. α-MG Reduces $NaIO_3$ Induced Intracellular ROS and Extracellular H_2O_2 Generation in ARPE-19 Cells

Previous research demonstrated that mitochondrial dysfunction induces the production of intracellular ROS [30]. We measured the levels of intracellular ROS using DCFH-DA (an intracellular ROS probe) and analyzed through flow cytometry. In agreement with the previous reports [8,25], treatment of the cultured cells with 6 mM of $NaIO_3$ caused approximately 60% cell death (Figure 1B) and an approximately 200% increase in intracellular ROS production (Figure 3A) respectively. Compared with the $NaIO_3$-treated group, pretreatment with α-MG attenuated the $NaIO_3$-induced intracellular ROS levels in the ARPE-19 cells (Figure 3A). We then measured the level of extracellular H_2O_2 using a commercial kit, and the results showed that the increased expression of H_2O_2 in the $NaIO_3$-induced group was significantly eliminated after treatment with α-MG (Figure 3B). These results established α-MG as an effective antioxidant against $NaIO_3$-induced oxidative stress by reducing ROS.

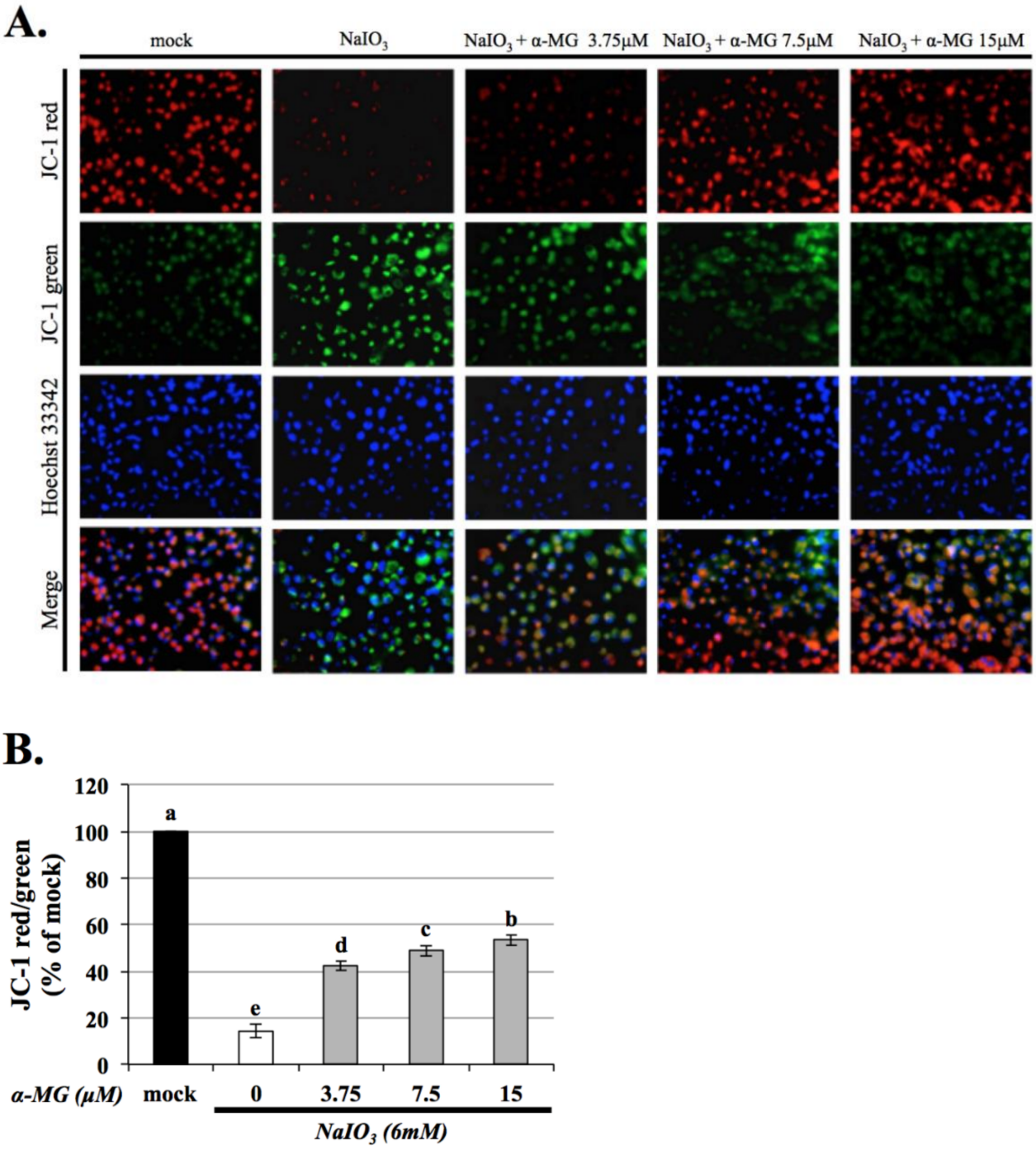

Figure 2. α-MG suppressed $NaIO_3$-induced mitochondrial dysfunction in ARPE-19 cells. (**A**) Representative images of staining with JC-1dye. The green areas represent the JC-1 monomer, which indicates impaired mitochondria, and the red areas represent the JC-1 polymer, which indicates healthy mitochondria. (**B**) Quantitative data obtained from the JC-1 staining assay. Data were expressed by mean ± SD ($n = 4$). Values without a common superscript letter are significantly different ($p < 0.05$).

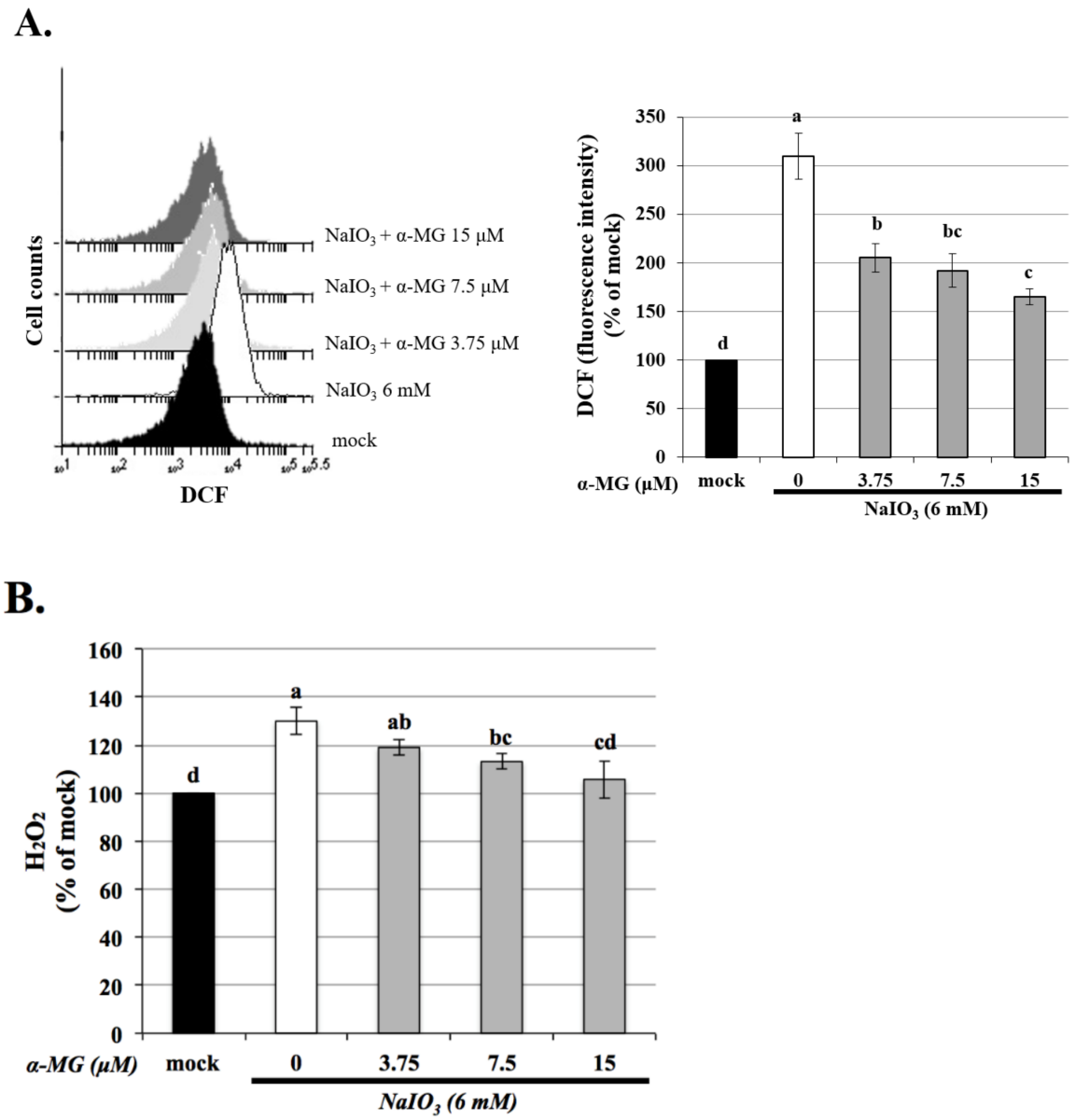

Figure 3. $NaIO_3$-induced intracellular ROS and extracellular H_2O_2 production in ARPE-19 cells was decreased by α-MG. Before $NaIO_3$ (6 mM) treatment, three different concentrations of α-MG (3.75, 7.5, and 15 μM) were pretreated to ARPE-19 cells for 1.5 h. Assessing the intracellular ROS (**A**) and H_2O_2 (**B**) generation level were detected by flowcytometry and commercial assay kits, respectively. Data were expressed by mean ± SD (n = 3). Values without a common superscript letter are significantly different ($p < 0.05$).

3.4. α-MG Improves $NaIO_3$-Induced Decreasing Antioxidant Status in ARPE-19 Cells

In mammals, the cellular ROS generation major occurs in mitochondria, which are also considered as the center of cellular bioenergetics. SOD2 is a mitochondrial antioxidant that helps to eliminate $O_2^{\bullet -}$ and induce the production of H_2O_2. However, if H_2O_2 cannot be metabolized, ROS will be produced. Antioxidant enzymes play a major role in ROS scavenging, and changes in their expression or/and activity are reported to be associated with AMD. As shown in Figure 4, the expressions of SOD activity were increased, but catalase and GSH were decreased in the $NaIO_3$-induced group. α-MG (7.5 and 15 μM) treatment significantly reversed the reduced levels of catalase and GSH and the increased level of SOD, indicating that α-MG could modulate the activity of antioxidants. These results suggested that α-MG decreased $NaIO_3$-induced oxidative stress by increasing intracellular antioxidant enzyme activity.

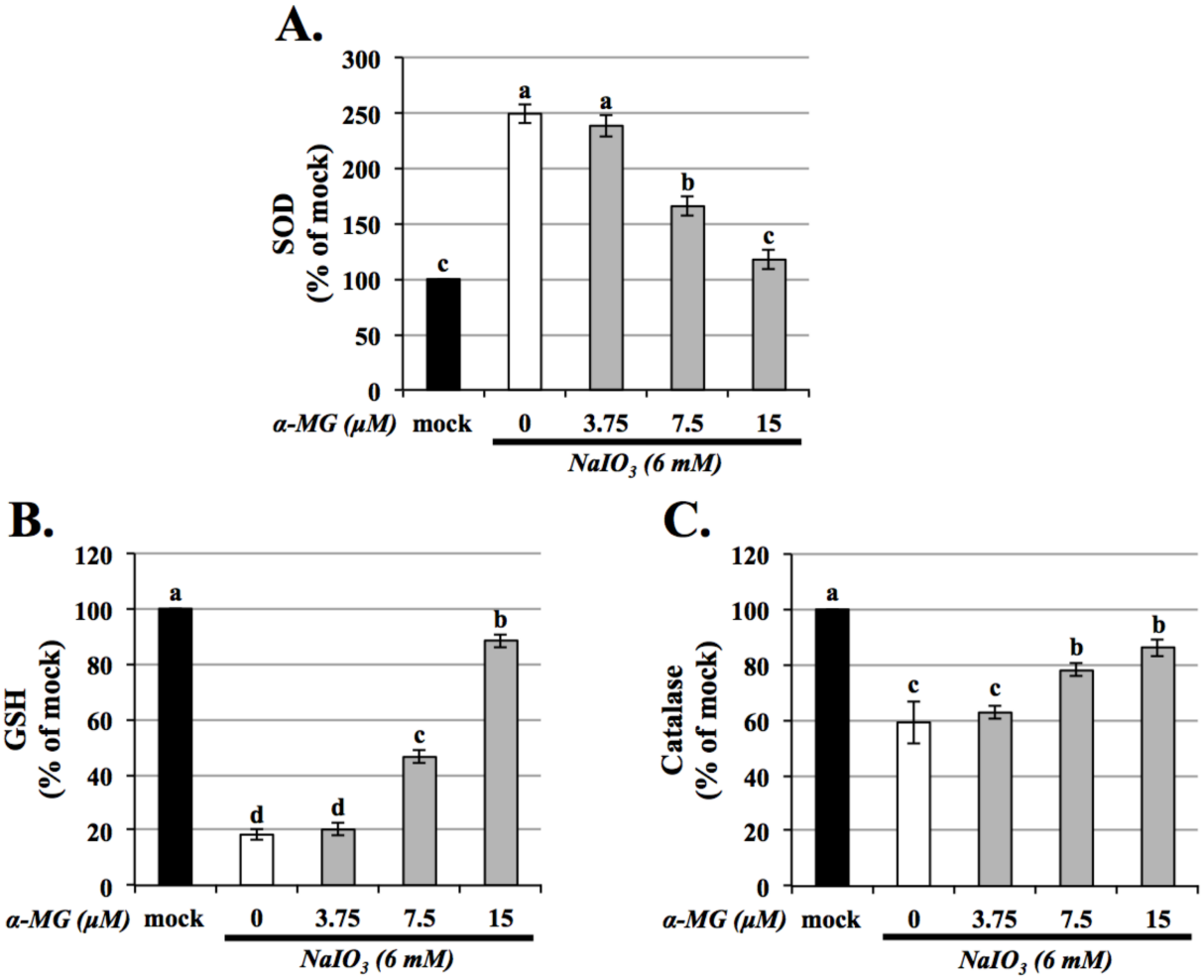

Figure 4. Effects of alpha-mangostin on the expression of SOD, GSH, and catalase levels in $NaIO_3$-induced ARPE-19 cells. Before $NaIO_3$ (6 mM) treatment, three different concentrations of α-MG (3.75, 7.5, and 15 μM) were pretreated to ARPE-19 cells for 1.5 h. The cell lysates were collected to assess the activities of SOD (**A**), glutathione (GSH) (**B**), and catalase (**C**) by commercial assay kits. Data were expressed by mean ± SD (n = 3). Values without a common superscript letter are significantly different ($p < 0.05$).

3.5. α-MG Protects $NaIO_3$-Induced Apoptosis in ARPE-19 Cells

Oxidative stress can induce cell apoptosis. To further investigate this protective effect of α-MG on the cell viability of ARPE-19 cells, the morphological change and apoptosis rate of ARPE-19 cells, incubated with α-MG (3.75, 7.5, and 15 μM) for 1.5 h, and then exposed to 6 mM $NaIO_3$ for 24 h, were determined under a microscope (Figure 5A) and by flow cytometry (Figure 5B), respectively. Consistently, exposure to 6 mM $NaIO_3$ led to a significantly higher rate of total apoptosis compared with that of the control group; however, pretreatment of ARPE-19 cells with α-MG at concentrations of 3.75, 7.5, and 15 μM before $NaIO_3$ exposure significantly decreased $NaIO_3$-induced cell apoptosis. These results confirmed that α-MG inhibiting ROS levels could rescue $NaIO_3$-induced retinal toxicity by apoptosis.

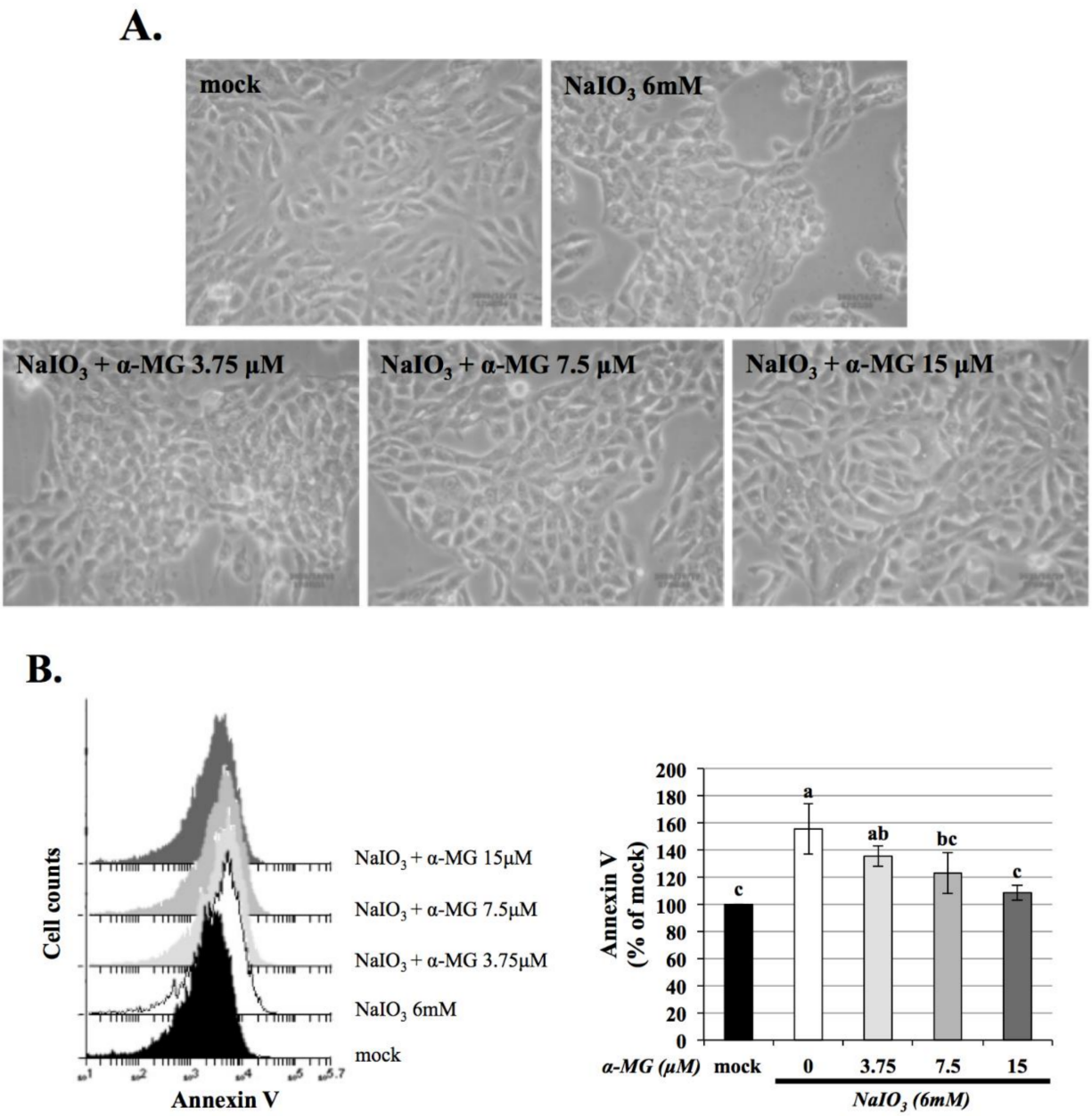

Figure 5. α-MG suppressed $NaIO_3$-induced ARPE-19 cell apoptosis. (**A**) Morphological images of ARPE-19 cells following different treatment. (**B**) ARPE-19 cells were pretreated with the indicated concentrations of α-MG (0, 3.75, 7.5, and 15 μM) for 1.5 h, followed by $NaIO_3$ (6 mM) administration for 24 h. Apoptosis was measured by flow cytometry using Annexin-V staining. Data were expressed by mean ± SD (n = 3). Values without a common superscript letter are significantly different ($p < 0.05$).

3.6. Effect of α-MG on Apoptotic-Related Protein Expression in $NaIO_3$-Treated ARPE-19 Cells

To confirm the protective effect of α-MG against $NaIO_3$-induced apoptosis in ARPE-19 cells, we further investigated the effects of α-MG on the expression of apoptosis-related molecules, i.e., Bcl-2, Bax, cleaved PARP-1, and cleaved caspase-3 by Western blotting (Figure 6). Compared with normal control cells, exposure to $NaIO_3$ induced lower levels of Bcl-2 and higher levels of Bax, cleaved PARP-1, and cleaved caspase-3. However, antioxidants of ARPE-19 cells with α-MG (3.75, 7.5 and 15 μM) for 1.5 h dose-dependently reversed this situation, as shown by the decreased expression of Bax, cleaved PARP-1, and cleaved caspase-3, as well as the increased expression of Bcl-2, which was statistically significant relative to those in $NaIO_3$ group.

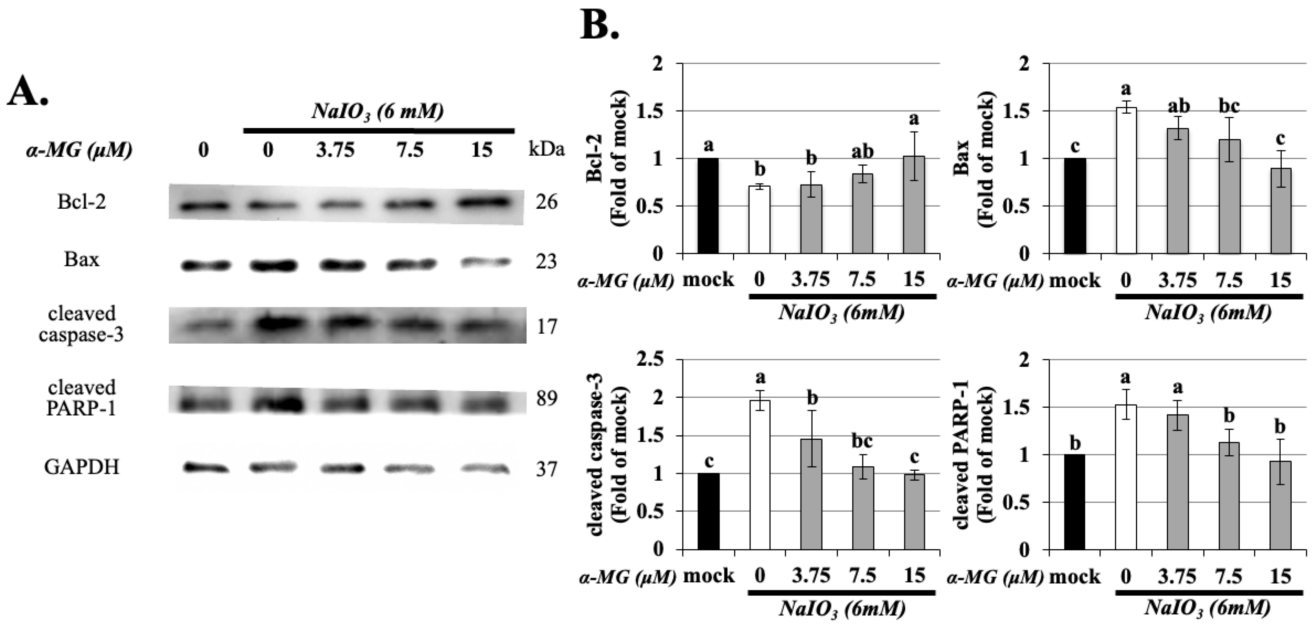

Figure 6. α-MG reduced the expressions of Bcl-2, Bax, cleaved caspase-3, and cleaved PARP-1 in $NaIO_3$-treated ARPE-19 cells. ARPE-19 cells were either untreated (mock) or treated with α-MG (0, 3.75, 7.5, and 15 μM) followed by $NaIO_3$ (6 mM). Total protein from the ARPE-19 cells was extracted for the measurement of Bcl-2, Bax, cleaved caspase-3, and cleaved PARP-1 expression using Western blot analysis (**A**). The quantified expressions of (**B**), as mean ± SD (n = 3, 3 individual set experiments of groups). GAPDH density was used as internal control to normalize all proteins expression levels. Values without a common superscript letter are significantly different ($p < 0.05$).

3.7. α-MG Downregulates PGC-1α and SIRT-3 Expression through the Inhibition of PI3K/AKT Signaling Pathway in $NaIO_3$-Treated ARPE-19 Cells

Sirtuin-3 (SIRT-3) is crucial for controlling mitochondrial metabolism and homeostasis and protects cells from death under conditions of stress [31]. Du et al. (2019) demonstrated that SIRT-3 was implicated in the effect of H_2O_2-induced RPE cell oxidative stress, autophagy, and apoptosis [32]. In this study, we assessed whether SIRT-3 was required for protection from ROS production in RPE cells during $NaIO_3$ treatment. To explore the protective mechanisms of α-MG, the PI3K/AKT signaling pathway and the expression of PGC-1α/ SIRT-3 were detected with western blot. The results suggested that the expression of PI3K and phosphorylation of AKT on ARPE-19 cells were significantly increased after 24 h of $NaIO_3$ treatment compared with the normal control group, which had been downregulated by α-MG (Figure 7A,B). Simultaneously, as shown in Figure 7C,D, a statistically significant increase in PGC-1α and SIRT-3 protein expression was shown in the $NaIO_3$ group. Along with the result of α-MG on the depression of PGC-1α and SIRT-3 protein levels, we found that α-MG protected RPE cells against $NaIO_3$-induced oxidative damage by reducing the SIRT-3 expression mediated by the PI3K/AKT/ PGC-1α signaling pathway.

3.8. α-MG Inhibition Preserves the Physiological Function of the Retina in Mice following $NaIO_3$ Treatment

To validate the role of α-MG in the pathogenesis of AMD in vivo, $NaIO_3$-injected mice were used as an animal mode [8,25]. We then performed optical coherence tomography (OCT), hematoxylin, and eosin staining to assess geographic atrophy in mice. Optical coherence tomography was performed to detect the effects of α-MG on the retina injuries induced by $NaIO_3$. The results showed that α-MG, at the end of the detection points, significantly decreased the thinning of the retina caused by $NaIO_3$ treatment (Figure 8A,B).

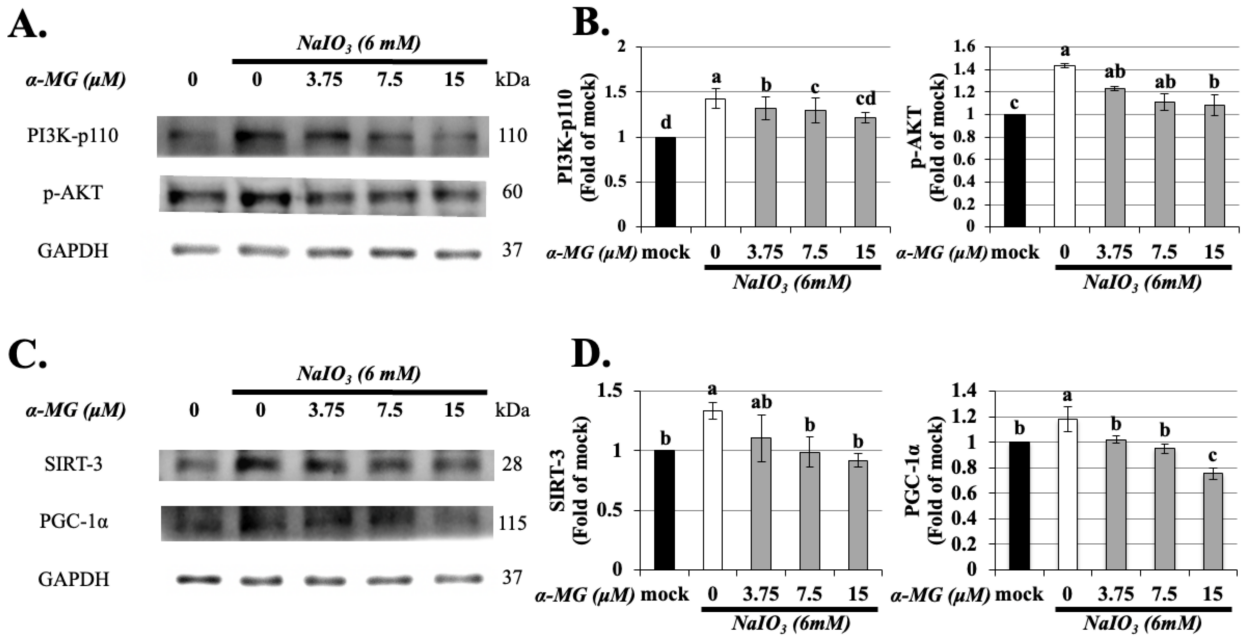

Figure 7. α-MG reduced the expressions of PI3K, p-AKT, SIRT-3, and PGC-1α in $NaIO_3$-treated ARPE-19 cells. ARPE-19 cells were either untreated (mock) or treated with α-MG (0, 3.75, 7.5, and 15 μM) followed by $NaIO_3$ (6 mM). Total protein from the ARPE-19 cells was extracted for the measurement of PI3K, p-AKT, SIRT-3, and PGC-1α expressions using Western blot analysis (**A**,**C**). The quantified expressions of (**B**,**D**), as mean ± SD (n = 3, 3 individual set experiments of groups). GAPDH density was used as internal control to normalize all proteins expression levels. Values without a common superscript letter are significantly different ($p < 0.05$).

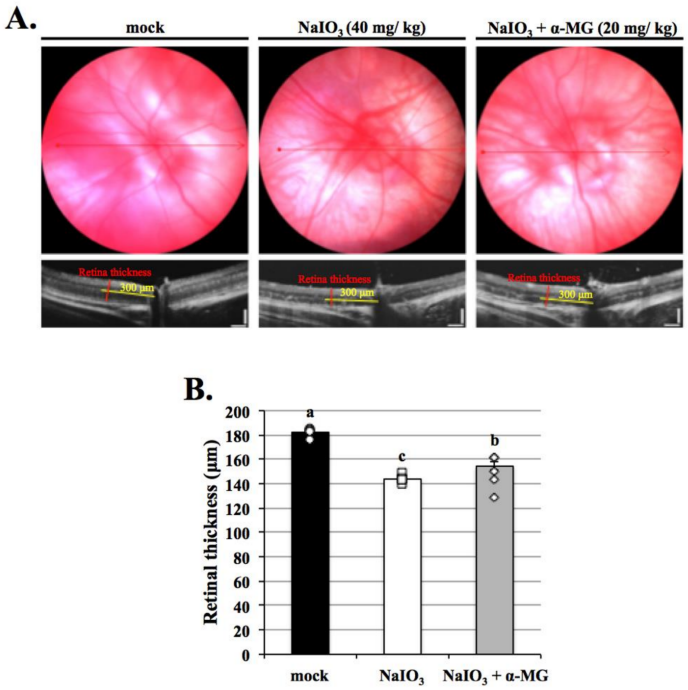

Figure 8. Effects of α-MG on the thinning of retinas in vivo. (**A**) Optical coherence tomography measurement of the effects of α-MG on retinas treated with $NaIO_3$ in mice. (**B**) There was significantly increased thinning of retinas in the $NaIO_3$ group compared with the mock group; however, α-MG significantly inhibited thinning of retinas after treatment of $NaIO_3$ on day seven, compared with the $NaIO_3$ groups. Data were measured by mean ± SD (n = 6). Values without a common superscript letter are significantly different ($p < 0.05$).

To further prove this, hematoxylin and eosin (H&E) staining was performed to detect the effects of α-MG on the pathological changes of retina after $NaIO_3$ administration. Alterations in retinal morphology began to appear seven days after $NaIO_3$ injection in mice, with a reduction in the outer nuclear layer (ONL) and inner nuclear layer (INL) (Figure 9). In contrast, α-MG moderated the alterations in retinal morphology by preserving the ONL and INL thickness of the retina after $NaIO_3$ administration. As shown in the graph of H&E staining, compared with the mock group, the thickness of INL and ONL were decreased by about 10–30 μm after the induction of $NaIO_3$, which could be reversed by about 10–20 μm with α-MG pretreatment. Collectively, our data show that α-MG mediates retinal degeneration in a dry AMD mouse model.

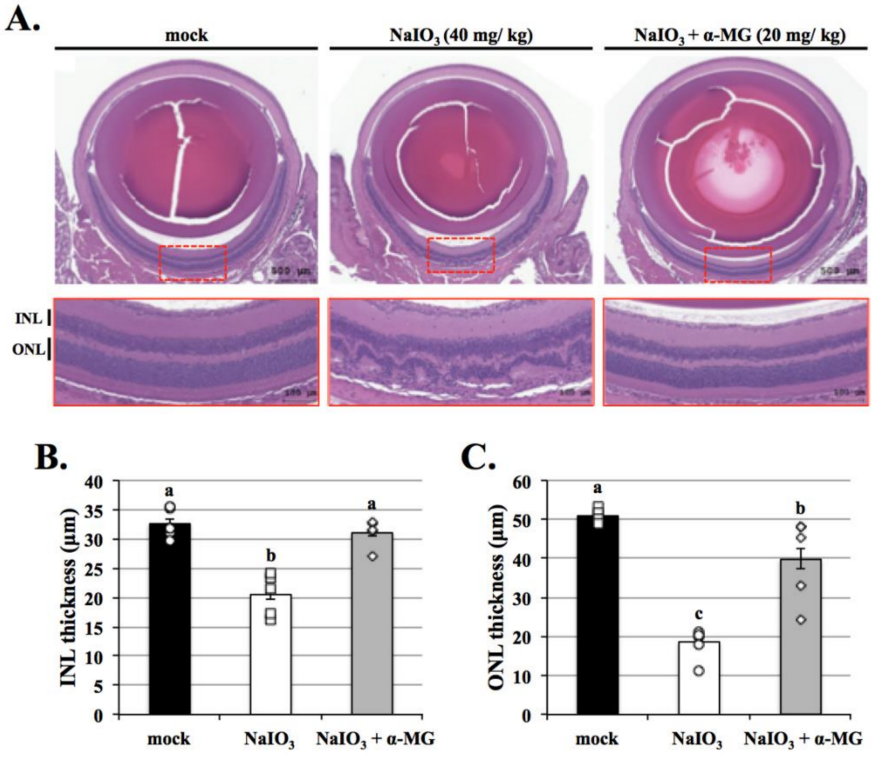

Figure 9. Protective effects of α-MG on retinal degeneration in $NaIO_3$-treated mice. (**A**) Different three retinal sections (H&E staining) from three groups were captured of the tissue section image via optical microscope (Olympus Optical, Tokyo, Japan). RPE, retinal pigment epithelium; IS-OS, inner and outer segment of photoreceptor; ONL, outer nuclear layer; INL, inner nuclear layer. Scale bar = 50 μm. There were marked six different positions to measure (**B**) INL and (**C**) ONL thickness were randomly measured 6 times between the range of 600–900 μm on nasal and temporal side of the optic nerve to take the average. Data were expressed by mean ± SD (n = 6). Values without a common superscript letter are significantly different ($p < 0.05$).

3.9. α-MG Reduced Apoptosis on Retinal Apoptosis Induced by $NaIO_3$ in Mice following $NaIO_3$ Treatment

Previous research has shown through in vitro studies that α-MG inhibiting ROS levels could rescue $NaIO_3$-induced retinal toxicity by apoptosis. Therefore, we further explored whether α-MG could inhibit the protective effect of $NaIO_3$-induced retinal cell damage by regulation cleaved caspase-3. We performed immunohistochemical staining on the cleaved caspase-3 after seven days of treated mice. The results showed that in the mock and α-MG groups, the expression level of cleaved caspase-3 was significantly lower in the $NaIO_3$-treated group (Figure 10).

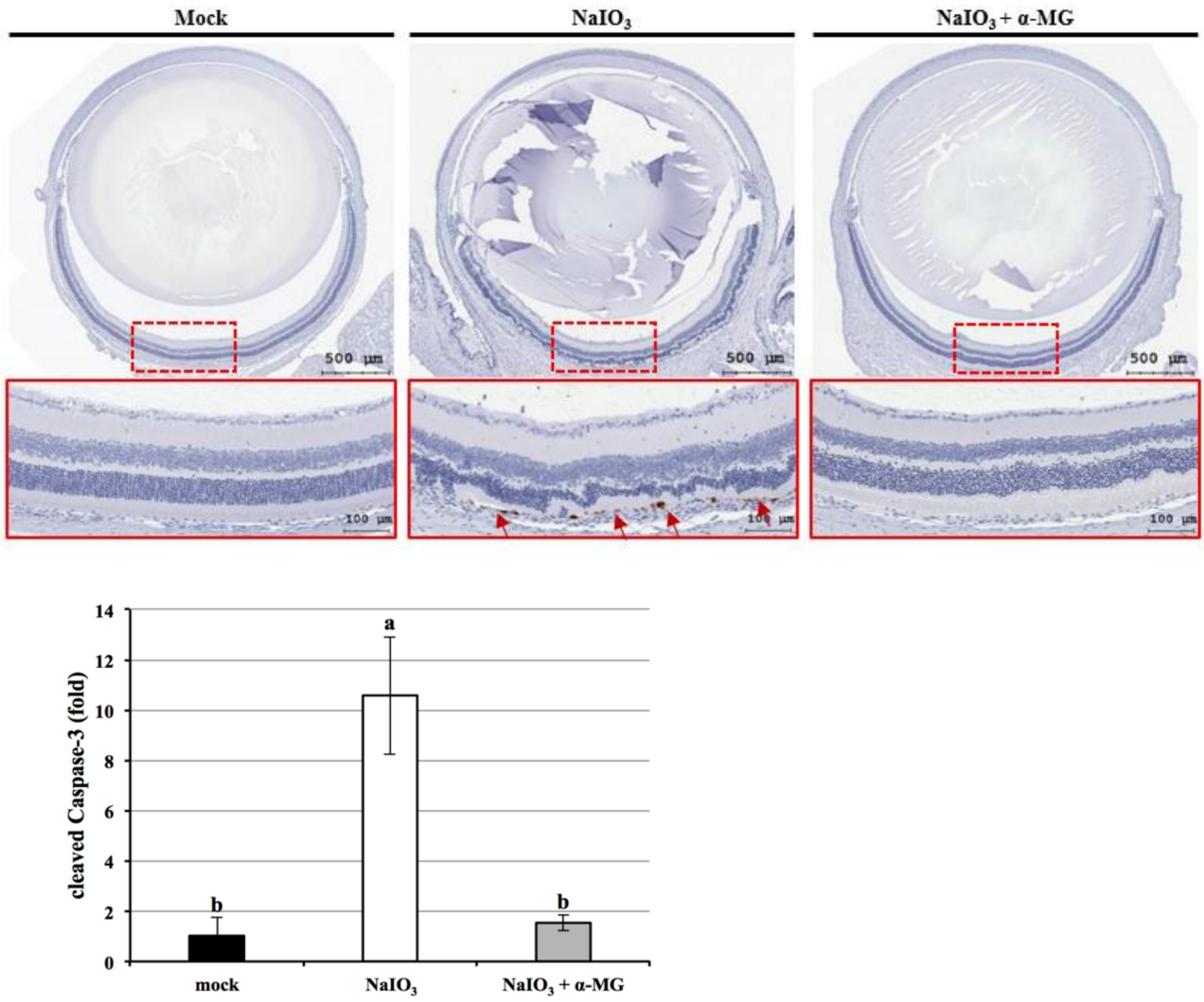

Figure 10. Effect of α-MG on $NaIO_3$-induced retinal cell damage via apoptosis in mice. All retinal sections in three study groups were collected after seven days of $NaIO_3$ treatment and stained with cleaved caspase-3 by immunohistochemical. Red arrows represent the performance of cleaved caspase-3 (brown) in retinal pigment epithelial (RPE) layers. Compared with mock and experimental ($NaIO_3$ + α-MG) groups, the $NaIO_3$ group expressed a significantly large amount of cleaved caspase-3. Data were expressed by mean ± SD (n = 6). Values without a common superscript letter are significantly different ($p < 0.05$).

4. Discussion

$NaIO_3$, as a kind of stable oxidant, has been shown to effectively induce retinal degeneration; this model is widely used because of its reproducibility and controllable degree of retinal damage [33]. $NaIO_3$-induced cell death in RPE cells is a valuable in vitro model of AMD. Although many studies using this model demonstrate the death features and molecular events underlying the oxidative stress-mediated cellular responses mimicking the pathogenesis of AMD, it remains unclear regarding ROS-mediated signaling pathways, mitochondrial function, autophagy, and mitophagy, which are integrated to control cell viability in RPE [8,25].

Excessive mitochondrial ROS are known to induce apoptosis. It is well known that the activity of GSH, SOD, and catalase protects cells against ROS-induced oxidative damage [34]. As shown in Figure 4, the expressions of antioxidants except SOD were dramatically decreased in the $NaIO_3$-induced group. α-MG treatment significantly reversed the reduced levels of catalase and GSH and the increased level of SOD, indicating that

α-MG could modulate the activity of antioxidants. Previous research reported that $NaIO_3$ induced cytosolic ROS production, but not mitochondrial ROS production; furthermore, it activated ERK, p38, JNK, and protein kinase B (AKT) signaling pathways [35]. Consistently, in our study, the cytosolic ROS production in the ARPE-19 cells was demonstrated under the $NaIO_3$-induced retinal degeneration, which was detected as intracellular ROS by DCFH-DA fluorescent probes (Figure 3) and extracellular H_2O_2 production. Additionally, we found that the induction of $NaIO_3$ also promoted mitochondrial damage via the relative intensities of green/red JC-1 fluorescence (Figure 2). These results indicate that α-MG could protect cells from $NaIO_3$-mediated ROS injury by maintaining ROS levels and mitochondrial disruption. In addition, in vivo, we found that α-MG significantly retarded the atrophy of $NaIO_3$-induced thickness of the total retina, INL, and ONL of $NaIO_3$-treated mice at seven days (Figure 9).

It is well known that PGC-1α participates in the regulation of mitochondrial function and redox state [36]. PGC-1α has been reported to be the upstream target gene of SIRT-1/3, indicating that PGC-1α can strongly stimulate SIRT-3 gene expression [37,38]. SIRT-3, a member of the sirtuin family, is localized in the mitochondria and plays pivotal roles in oxidative pathways by targeting several enzymes [39]. SIRT-3 plays important roles in the inhibition of oxidative stress-induced retinal cell death in early diabetic rats [40]. We observed that α-MG treatment decreased PGC-1α and SIRT-3 expression in $NaIO_3$-induced RPE cells (Figure 7C,D). With this result, we prove that PGC-1α and SIRT-3 are related to the effects of $NaIO_3$-induced oxidative stress and apoptosis in RPE cells in vitro, but the treatment of α-MG can attenuate this appearance. Consequently, this study showed the capacity of α-MG on $NaIO_3$-induced RPE cell oxidative stress and apoptosis and the importance of SIRT-3 on mitochondrial ROS regulation in ARPE-19 cells. Finally, we confirmed by the activated PI3K/AKT-PGC-1α signaling pathway that the expression of SIRT-3 was involved in the action of α-MG on RPE cell apoptosis.

In our previous studies, Chang et al. (2021) and Chan et al. (2019), we reported that $NaIO_3$-induced PI3K/AKT activation was partially dependent on ROS production, eventually leading to cell death by apoptosis [25,41]. These results indicate that $NaIO_3$ induces apoptosis by increasing the cleaved form of caspase-3, PARP-1, and the Bax/Bcl-2 ratio in RPE cells. In addition, we found that α-MG significantly reduced the production of $NaIO_3$-induced cleaved caspase-3 expression by in vivo (Figure 10).

In this study, we found that α-MG inhibited $NaIO_3$-induced cell apoptosis by mediating PI3K/AKT inactivation (Figure 7), thereby downregulating the expressions of Bax, cleaved caspase-3, and cleaved PARP and upregulating Bcl-2 expression (Figure 6). The results of this study show that α-MG significantly protected ARPE-19 cells against $NaIO_3$-induced toxicity, high ROS levels, and apoptosis in vitro. Most importantly, the results of this study, for the first time, support a model whereby α-MG inhibits PI3K/AKT-PGC-1α signaling, which is required for the regulation of SIRT-3 protein expression (Figure 11).

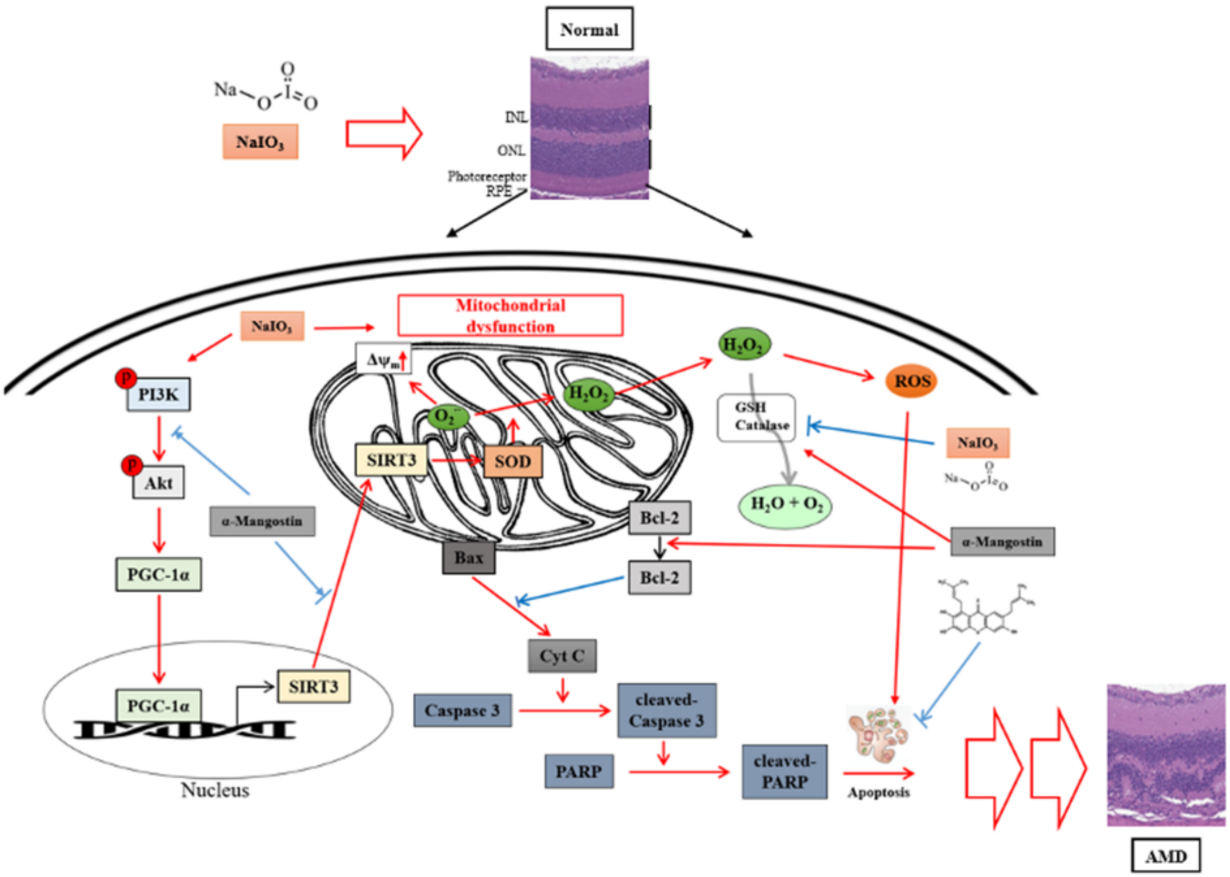

Figure 11. The possible role of α-MG on attenuating sodium iodate-induced RPE cells cytotoxicity and retinal oxidative injury.

5. Conclusions

In summary, our in vitro and in vivo experimental results showed that α-MG could protect retinal cells (especially RPE cells) from oxidative stress damage via apoptosis. The protective function of α-MG on oxidative stressed RPE cells is expressed through its antiapoptotic effect. As a result, α-MG may be able to serve as a potent therapeutic agent for the treatment of retinal degeneration diseases.

Author Contributions: H.-W.L. and Y.-Y.C. conceived and designed the experiments. C.-J.C., M.W., J.-H.Y., T.-C.C., Y.-J.L. and S.-C.T. performed the experiments and wrote the manuscript. C.-J.C., M.W., J.-H.Y., T.-C.C., Y.-J.L. and S.-C.T. provided help during the data analysis. All authors have read and agreed to the published version of the manuscript.

Funding: The authors would like to thank the Chung Shan Medical University (project numbers: NCHU-CSMU-10708, and NCHU-CSMU-10910), and the Ministry of Science and Technology, Taiwan (project numbers: MOST-108-2320-B-468-002, MOST-109-2320-B-040-019-MY3, and MOST-109-2320-B-468-004-MY3) for financially supporting this research.

Institutional Review Board Statement: All animal use protocols in this study were approved by Institutional Animal Care and Use Committee at the Chung Shan Medical University (IACUC approval number: 2262) and all investigations were carried out following the "Guide to the Care and Use of Experimental Animals".

Informed Consent Statement: Not applicable.

Data Availability Statement: Data are contained within the article.

Conflicts of Interest: The authors declare no conflict of interest.

References

1. Wang, Z.Y.; Shen, L.J.; Tu, L.; Hu, D.N.; Liu, G.Y.; Zhou, Z.L.; Lin, Y.; Chen, L.H.; Qu, J. Erythropoietin protects retinal pigment epithelial cells from oxidative damage. *Free Radic. Biol. Med.* **2009**, *46*, 1032–1041. [CrossRef] [PubMed]
2. Winkler, B.S.; Boulton, M.E.; Gottsch, J.D.; Sternberg, P. Oxidative damage and age-related macular degeneration. *Mol. Vis.* **1999**, *5*, 32.
3. Buschini, E.; Fea, A.M.; Lavia, C.A.; Nassisi, M.; Pignata, G.; Zola, M.; Grignolo, F.M. Recent developments in the management of dry age-related macular degeneration. *Clin. Ophthalmol.* **2015**, *9*, 563–574. [CrossRef]
4. Ding, X.; Patel, M.; Chan, C.C. Molecular pathology of age-related macular degeneration. *Prog. Retin. Eye Res.* **2009**, *28*, 1–18. [CrossRef] [PubMed]
5. Wang, K.; Jiang, Y.; Wang, W.; Ma, J.; Chen, M. Escin activates AKT-Nrf2 signaling to protect retinal pigment epithelium cells from oxidative stress. *Biochem. Biophys. Res. Commun.* **2015**, *468*, 541–547. [CrossRef] [PubMed]
6. Cao, G.-F.; Liu, Y.; Yang, W.; Wan, J.; Yao, J.; Wan, Y.; Jiang, Q. Rapamycin sensitive mTOR activation mediates nerve growth factor (NGF) induced cell migration and pro-survival effects against hydrogen peroxide in retinal pigment epithelial cells. *Biochem. Biophys. Res. Commun.* **2011**, *414*, 499–505. [CrossRef]
7. Yao, J.; Bi, H.-E.; Sheng, Y.; Cheng, L.-B.; Wendu, R.-L.; Wang, C.-H.; Cao, G.-F.; Jiang, Q. Ultraviolet (UV) and hydrogen peroxide activate ceramide-ER stress-AMPK signaling axis to promote retinal pigment epithelium (RPE) cell apoptosis. *Int. J. Mol. Sci.* **2013**, *14*, 10355–10368. [CrossRef] [PubMed]
8. Hsu, M.-Y.; Hsiao, Y.-P.; Lin, Y.-T.; Chen, C.; Lee, C.-M.; Liao, W.-C.; Tsou, S.-C.; Lin, H.-W.; Chang, Y.-Y. Quercetin Alleviates the Accumulation of Superoxide in Sodium Iodate-Induced Retinal Autophagy by Regulating Mitochondrial Reactive Oxygen Species Homeostasis through Enhanced Deacetyl-SOD2 via the Nrf2-PGC-1α-Sirt1 Pathway. *Antioxidants* **2021**, *10*, 1125. [CrossRef]
9. Shamsi, F.A.; Chaudhry, I.A.; Boulton, M.E.; Al-Rajhi, A.A. L-carnitine protects human retinal pigment epithelial cells from oxidative damage. *Curr. Eye Res.* **2007**, *32*, 575–584. [CrossRef] [PubMed]
10. Baldelli, S.; Aquilano, K.; Ciriolo, M.R. PGC-1α buffers ROS-mediated removal of mitochondria during myogenesis. *Cell Death Dis.* **2014**, *5*, e1515. [CrossRef]
11. Salminen, A.; Kaarniranta, K.; Kauppinen, A. Crosstalk between Oxidative Stress and SIRT1: Impact on the Aging Process. *Int. J. Mol. Sci.* **2013**, *14*, 3834–3859. [CrossRef] [PubMed]
12. Iacovelli, J.; Rowe, G.C.; Khadka, A.; Diaz-Aguilar, D.; Spencer, C.; Arany, Z.; Saint-Geniez, M. PGC-1α Induces Human RPE Oxidative Metabolism and Antioxidant Capacity. *Investig. Ophthalmol. Vis. Sci.* **2016**, *57*, 1038–1051. [CrossRef]
13. Song, C.; Zhao, J.; Fu, B.; Li, D.; Mao, T.; Peng, W.; Wu, H.; Zhang, Y. Melatonin-mediated upregulation of Sirt3 attenuates sodium fluoride-induced hepatotoxicity by activating the MT1-PI3K/AKT-PGC-1α signaling pathway. *Free. Radic. Biol. Med.* **2017**, *112*, 616–630. [CrossRef] [PubMed]
14. Wang, M.H.; Zhang, K.J.; Gu, Q.L.; Bi, X.L.; Wang, J.X. Pharmacology of mangostins and their derivatives: A comprehensive review. *Chin. J. Nat. Med.* **2017**, *15*, 81–93. [CrossRef]
15. Chen, L.G.; Yang, L.L.; Wang, C.C. Anti-inflammatory activity of mangostins from *Garcinia mangostana*. *Food Chem. Toxicol.* **2008**, *46*, 688–693. [CrossRef] [PubMed]
16. Liu, C.W.; Lin, H.W.; Yang, D.J.; Chen, S.Y.; Tseng, J.K.; Chang, T.J.; Chang, Y.Y. Luteolin inhibits viral-induced inflammatory response in RAW264.7 cells via suppression of STAT1/3 dependent NF-κB and activation of HO-1. *Free Radic. Biol. Med.* **2016**, *95*, 180–189. [CrossRef] [PubMed]
17. Nelli, G.B.; K, A.S.; Kilari, E.K. Antidiabetic effect of α-mangostin and its protective role in sexual dysfunction of streptozotocin induced diabetic male rats. *Syst. Biol. Reprod. Med.* **2013**, *59*, 319–328. [CrossRef]
18. Sivaranjani, M.; Prakash, M.; Gowrishankar, S.; Rathna, J.; Pandian, S.K.; Ravi, A.V. In vitro activity of alpha-mangostin in killing and eradicating *Staphylococcus epidermidis* RP62A biofilms. *Appl. Microbiol. Biotechnol.* **2017**, *101*, 3349–3359. [CrossRef] [PubMed]
19. Jung, H.A.; Su, B.N.; Keller, W.J.; Mehta, R.G.; Kinghorn, A.D. Antioxidant xanthones from the pericarp of *Garcinia mangostana* (Mangosteen). *J. Agric. Food Chem.* **2006**, *54*, 2077–2082. [CrossRef] [PubMed]
20. Akao, Y.; Nakagawa, Y.; Iinuma, M.; Nozawa, Y. Anti-cancer effects of xanthones from pericarps of mangosteen. *Int. J. Mol. Sci.* **2008**, *9*, 355–370. [CrossRef]
21. Mohamed, G.A.; Al-Abd, A.M.; El-Halawany, A.M.; Abdallah, H.M.; Ibrahim, S.R.M. New xanthones and cytotoxic constituents from *Garcinia mangostana* fruit hulls against human hepatocellular, breast, and colorectal cancer cell lines. *J. Ethnopharmacol.* **2017**, *198*, 302–312. [CrossRef] [PubMed]
22. Devi Sampath, P.; Vijayaraghavan, K. Cardioprotective effect of alpha-mangostin, a xanthone derivative from mangosteen on tissue defense system against isoproterenol-induced myocardial infarction in rats. *J. Biochem. Mol. Toxicol.* **2007**, *21*, 336–339. [CrossRef] [PubMed]
23. Cui, J.; Hu, W.; Cai, Z.; Liu, Y.; Li, S.; Tao, W.; Xiang, H. New medicinal properties of mangostins: Analgesic activity and pharmacological characterization of active ingredients from the fruit hull of *Garcinia mangostana* L. *Pharmacol. Biochem. Behav.* **2010**, *95*, 166–172. [CrossRef] [PubMed]
24. Márquez-Valadez, B.; Lugo-Huitrón, R.; Valdivia-Cerda, V.; Miranda-Ramírez, L.R.; Pérez-De La Cruz, V.; González-Cuahutencos, O.; Rivero-Cruz, I.; Mata, R.; Santamaría, A.; Pedraza-Chaverrí. J. The natural xanthone alpha-mangostin reduces oxidative damage in rat brain tissue. *Nutr. Neurosci.* **2009**, *12*, 35–42. [CrossRef] [PubMed]

25. Chang, Y.-Y.; Lee, Y.-J.; Hsu, M.-Y.; Wang, M.; Tsou, S.-C.; Chen, C.-C.; Lin, J.-A.; Hsiao, Y.-P.; Lin, H.-W. Protective Effect of Quercetin on Sodium Iodate-Induced Retinal Apoptosis through the Reactive Oxygen Species-Mediated Mitochondrion-Dependent Pathway. *Int. J. Mol. Sci.* **2021**, *22*, 4056. [CrossRef] [PubMed]
26. Moriguchi, M.; Nakamura, S.; Inoue, Y.; Nishinaka, A.; Nakamura, M.; Shimazawa, M.; Hara, H. Irreversible Photoreceptors and RPE Cells Damage by Intravenous Sodium Iodate in Mice Is Related to Macrophage Accumulation. *Investig. Ophthalmol. Vis. Sci.* **2018**, *59*, 3476–3487. [CrossRef] [PubMed]
27. Patil, P.; Agrawal, M.; Almelkar, S.; Jeengar, M.K.; More, A.; Alagarasu, K.; Kumar, N.V.; Mainkar, P.S.; Parashar, D.; Cherian, S. In vitro and in vivo studies reveal α-Mangostin, a xanthonoid from *Garcinia mangostana*, as a promising natural antiviral compound against chikungunya virus. *Virol. J.* **2021**, *18*, 47. [CrossRef]
28. Latendresse, J.R.; Warbrittion, A.R.; Jonassen, H.; Creasy, D.M. Fixation of testes and eyes using a modified Davidson's fluid: Comparison with Bouin's fluid and conventional Davidson's fluid. *Toxicol. Pathol.* **2002**, *30*, 524–533. [CrossRef] [PubMed]
29. Hou, S.; Song, Y.; Sun, D.; Zhu, S.; Wang, Z. Xanthohumol-Induced Rat Glioma C6 Cells Death by Triggering Mitochondrial Stress. *Int. J. Mol. Sci.* **2021**, *22*, 4506. [CrossRef] [PubMed]
30. Szeto, H.H. Pharmacologic Approaches to Improve Mitochondrial Function in AKI and CKD. *J. Am. Soc. Nephrol.* **2017**, *28*, 2856–2865. [CrossRef]
31. Kim, H.; Lee, Y.D.; Kim, H.J.; Lee, Z.H.; Kim, H.H. SOD2 and Sirt3 Control Osteoclastogenesis by Regulating Mitochondrial ROS. *J. Bone Miner. Res.* **2017**, *32*, 397–406. [CrossRef]
32. Du, Z.; Zhang, W.; Wang, S.; Zhang, J.; He, J.; Wang, Y.; Dong, Y.; Huo, M. Celastrol protects human retinal pigment epithelial cells against hydrogen peroxide mediated oxidative stress, autophagy, and apoptosis through sirtuin 3 signal pathway. *J. Cell. Biochem.* **2019**, *120*, 10413–10420. [CrossRef] [PubMed]
33. Enzmann, V.; Row, B.W.; Yamauchi, Y.; Kheirandish, L.; Gozal, D.; Kaplan, H.J.; McCall, M.A. Behavioral and anatomical abnormalities in a sodium iodate-induced model of retinal pigment epithelium degeneration. *Exp. Eye Res.* **2006**, *82*, 441–448. [CrossRef] [PubMed]
34. Thirupathi, A.; de Souza, C.T. Multi-regulatory network of ROS: The interconnection of ROS, PGC-1 alpha, and AMPK-SIRT1 during exercise. *J. Physiol. Biochem.* **2017**, *73*, 487–494. [CrossRef] [PubMed]
35. Hwang, N.; Kwon, M.Y.; Woo, J.M.; Chung, S.W. Oxidative Stress-Induced Pentraxin 3 Expression Human Retinal Pigment Epithelial Cells is Involved in the Pathogenesis of Age-Related Macular Degeneration. *Int. J. Mol. Sci.* **2019**, *20*, 6028. [CrossRef]
36. Wu, Z.; Puigserver, P.; Andersson, U.; Zhang, C.; Adelmant, G.; Mootha, V.; Troy, A.; Cinti, S.; Lowell, B.; Scarpulla, R.C.; et al. Mechanisms controlling mitochondrial biogenesis and respiration through the thermogenic coactivator PGC-1. *Cell* **1999**, *98*, 115–124. [CrossRef]
37. Kong, X.; Wang, R.; Xue, Y.; Liu, X.; Zhang, H.; Chen, Y.; Fang, F.; Chang, Y. Sirtuin 3, a new target of PGC-1alpha, plays an important role in the suppression of ROS and mitochondrial biogenesis. *PLoS ONE* **2010**, *5*, e11707. [CrossRef]
38. Gao, J.; Zhang, K.; Wang, Y.; Guo, R.; Liu, H.; Jia, C.; Sun, X.; Wu, C.; Wang, W.; Du, J.; et al. A machine learning-driven study indicates emodin improves cardiac hypertrophy by modulation of mitochondrial SIRT3 signaling. *Pharmacol. Res.* **2020**, *155*, 104739. [CrossRef]
39. Schwer, B.; North, B.J.; Frye, R.A.; Ott, M.; Verdin, E. The human silent information regulator (Sir)2 homologue hSIRT3 is a mitochondrial nicotinamide adenine dinucleotide-dependent deacetylase. *J. Cell Biol.* **2002**, *158*, 647–657. [CrossRef]
40. Zeng, Y.; Yang, K.; Wang, F.; Zhou, L.; Hu, Y.; Tang, M.; Zhang, S.; Jin, S.; Zhang, J.; Wang, J.; et al. The glucagon like peptide 1 analogue, exendin-4, attenuates oxidative stress-induced retinal cell death in early diabetic rats through promoting Sirt1 and Sirt3 expression. *Exp. Eye Res.* **2016**, *151*, 203–211. [CrossRef]
41. Chan, C.M.; Huang, D.Y.; Sekar, P.; Hsu, S.H.; Lin, W.W. Correction to: Reactive oxygen species-dependent mitochondrial dynamics and autophagy confer protective effects in retinal pigment epithelial cells against sodium iodate-induced cell death. *J. Biomed. Sci.* **2019**, *26*, 66. [CrossRef] [PubMed]